J Mater Sci (2019) 54:3847–3862

Composites

Improvement of mechanical properties and thermal conductivity of carbon fiber laminated composites through depositing graphene nanoplatelets on fibers

Fuzhong Wang[1,*] and Xiaoxia Cai[1]

[1] *Advanced Materials Institute, School of Materials Science and Engineering, Qilu University of Technology (Shandong Academy of Sciences), Jinan 250353, China*

Received: 2 October 2018
Accepted: 31 October 2018
Published online: 5 November 2018

ABSTRACT

In this study, a graphene nanoplatelets (GnPs)/acetone solution containing a small amount of resin/hardener was prepared as the spraying solution for modifying dry fabrics which are well compatible with the vacuum-assisted resin transfer infusion (VARI) process, and the GnPs-reinforced fiber laminated composites with GnPs uniformly distributed in the interlaminar regions were successfully fabricated. The results showed that the GnPs are well immobilized on the surface of carbon fibers after spray coating, and the mechanical properties and thermal conductivity of the carbon fiber/epoxy composites were effectively improved. The incorporation of 0.3 wt% GnPs produced the largest flexural strength and interlaminar shear strength, and the reinforcing mechanisms as well as failure modes of the composites were proposed. It was also noticed that the through-plane thermal conductivity of the composites consistently increases with increasing GnPs content due to the formation of effective conductive pathways between the interplies. The study suggested that the developed up-scalable spraying technique is an effective approach to deposit GnPs on dry carbon fabrics which are compatible with the economical VARI process for producing GnPs/fiber/epoxy multiscale composites with enhanced properties.

Introduction

Carbon fiber-reinforced plastics (CFRP) composites have been widely used in aerospace, automotive, construction, marine and sports equipment industries over the past few decades, due to their high specific strength and stiffness, excellent manufacturability and corrosion resistance [1–3]. In general, the in-plane properties of CFRP laminated composites are sufficient for many structural applications because of the high-performance fibers in the in-plane direction, while the out-of-plane/through-thickness properties, such as interlaminar shear strength (ILSS) and out-of-plane thermal conductivity, are affected by matrix and fiber/matrix interface

Address correspondence to E-mail: fullblownwang@hotmail.com

https://doi.org/10.1007/s10853-018-3097-3

adhesion which limited the applications of CFRP in many fields [4, 5].

In recent years, to meet the rising demand for high load-bearing structural composites and applications that require anti-lighting strike and heat dissipation, the introduction of carbonaceous nanomaterials into CFRP composites to create hierarchical structures and enhance the mechanical and physical properties has drawn considerable attention. Especially, the advantage of using carbon nanotubes (CNTs) as functional fillers in polymer composites has been extensively investigated due to their outstanding properties [6–8]. For example, El Moumen et al. [9–12] fabricated CNTs/fiber/epoxy composites by interleaving pre-prepared CNTs/epoxy films between carbon fabrics and systematically explored the effect of CNTs on the elastic modulus, fracture toughness, open-hole tension, shear beam, flatwise tension and impact properties of laminated composites. Promising outcomes encouraged more and more researchers to devote their efforts to fabricate composites with ultimate properties by employing suitable nanofillers and manufacturing processes. More recently, graphene has attracted a great deal of scientific interest due to its exceptional, structural and physical properties which include high aspect ratio, unique mechanical, electrical and thermal properties [13–15]. Many researchers have explored approaches to improve the interfacial properties of fiber-reinforced composites by using graphene oxide (GO) owing to the abundant oxygen-containing groups on GO. The ILSS, interfacial shear strength (IFSS) and mode I fracture toughness of the fiber-reinforced composites were reported to be effectively enhanced after the introduction of GO through modifying resins or continuous fibers with GO [16–18]. Based on the encouraging results, it is believed that the incorporation of conductive graphene instead of GO would not only enhance the interfacial properties but also be able to endow the composites with multifunctional properties.

Graphene nanoplatelets (GnPs) consisting of a few layers of graphene sheets can be produced at a relatively low cost through a top-down approach including mechanical exfoliation and liquid-phase exfoliation of pre-treated graphite [19–21]. The multilayer graphene sheets were reported to be superior to monolayer sheet in improving the thermal conductivity of the epoxy matrix [22], and our previous study also showed that the GnPs with larger aspect ratio generally demonstrate a higher thermal conductivity [23]. The GnPs are regarded as a type of true nanofiller for modifying polymer composites because of their excellent properties and low costs [23, 24]. Qin et al. [25] coated carbon fibers with GnPs (< 1 μm in diameter) by immersing carbon fibers in a GnPs suspension and fabricated GnPs-coated CF/epoxy composites by a prepreg and layup method. The hybrid composites exhibited 7% and 19% enhancements in flexural strength and ILSS, respectively, compared with the non-coated fiber composites. In addition, the through-thickness electrical conductivity of the resulting composites was significantly enhanced. Ahmadi-Moghadam et al. [26] reported that the mode I fracture toughness of the glass fiber/epoxy composites were obviously increased by introducing GnPs-reinforced epoxy resin into fabrics. The literature review suggested the good effectiveness of GnPs in enhancing the properties of laminated composites. To promote and extend the applications of GnPs/fiber/epoxy multiscale composites, it is important to develop time and cost-effective processing techniques which are easier to scale up to industrial production. The vacuum-assisted resin transfer infusion (VARI) process has been developed over the last decade to produce CFRP with low cost and high performances [27, 28]. The process has advantages over conventional resin transfer molding (RTM) since it employs low-cost one-sided mold and infuses dry fiber preform with low-viscosity resin under vacuum pressure. However, it is a challenge to employ VARI to fabricate GnPs-reinforced fiber laminated composites because the incorporation of GnPs into the resin would increase the viscosity of matrix and lead to weak fluidity, making the infiltration of carbon fabrics preform difficult in the subsequent resin infusion process. More importantly, filtration of the GnPs at the resin inlet by the fiber preform could lead to filler accumulation, resulting in inhomogeneous distribution of GnPs [29].

It is of great interest and important to uniformly introduce GnPs to CFRP with a facile approach which is compatible with the efficient and economical VARI process that can be implemented on an industrial scale. The introduction of fillers through spraying fillers on dry fibers is particularly interesting as it may overcome the issues of filtration and viscosity, while the modified fibers are usually not well compatible with the VARI process because the fillers

loosely attached to fibers may be easily washed off during the impregnation process, which resulted in limited reinforcing effect [30]. There have been some reports on the fabrication and mechanical properties of graphene/GO-reinforced fiber laminated composites [25, 31, 32]. However, the employment of using the spraying technique to transfer GnPs to dry fabrics that are compatible with the VARI process for producing CFRP has been rarely reported.

In this study, a GnPs/acetone solution containing a small amount of resin/hardener was prepared as a modified spraying solution, and an easily up-scalable spraying technique was used to develop novel GnPs-coated fiber fabrics which are well compatible with the VARI process for producing GnPs/fiber/epoxy multiscale composites with GnPs uniformly distributed in the interlaminar regions. The presence of resin/hardener in the spraying solution could assist the dispersion of GnPs in solution, and after spray coating, the GnPs could be well anchored on the fiber surface with the aid of the partially cured resins which can prevent the GnPs from immigrating and forming aggregates during the following VARI process. The aim of the current work is to transfer GnPs to the fiber surface with the spraying technique and produce GnPs-reinforced fiber laminated composites via the VARI process and then assess the ability of GnPs to enhance the mechanical properties and thermal conductivity of the resulting composites. This study will open new horizons of preparing GnPs/fiber/epoxy multiscale composites with a facial approach which is feasible scale-up for real industrial production.

Experimental

Materials

Unidirectional carbon fabric with the fiber areal weight of 196 g/m^2 (Hengshen Co., Ltd., Jiangsu, China) was employed to fabricate the CFRP laminates, where the diameter of carbon fiber (CF) was 7 μm. The GnPs with a specific surface area of 150 m^2/g used in this research had an average thickness of 5 nm and an average particle diameter of 5 μm, obtained from the XG Sciences (Lansing, MI). Araldite LY1564 (Bisphenol A) epoxy resin was used throughout this study, along with Aradur 3486 (Cycloaliphatic polyamine) hardener, which was supplied by the Huntsman Co. (West Point, GA, USA). Acetone was ordered from Avantor Performance Materials Inc, Center Valley, Pennsylvania, USA. All chemicals were used as received unless otherwise stated.

Experimental methods

Preparation of GnPs suspensions

To disperse the GnPs into a solvent for spray coating, 30.0 g Araldite LY1564 epoxy resin and 2.55 g Aradur 3486 were dissolved into 500 ml acetone, followed by adding measured quantities of GnPs. After that, the mixture was stirred by a high-speed magnetic stirrer for 5 min and then sonicated using a tip sonicator for 15 min at a power of 100 W. Subsequently, the resulting mixture was further treated under high shear forces using a digital shear disperser (IKA T25, Germany) for 5 min at 13,600 rpm. Finally, a homogeneous suspension containing GnPs at a concentration of 2 mg/ml was produced.

Specimen manufacturing

A high atomizing spray gun connected with a air compressor with a nozzle size of 0.5 mm was employed in this work to uniformly spray GnPs onto carbon fabrics. Prior to spraying, the carbon fiber cloth was cut into pieces with dimensions of 15 cm × 15 cm using a laser cutting machine which can avoid disturbing the fiber alignments. During spray coating, the spray gun was positioned perpendicular to the fabric so as to achieve homogeneous dispersion. The distance between spraying nozzle and the carbon fabric was kept at 15 cm, and the optimized spraying air pressure was set at 5.0 bar during deposition. A heating stage with a controlled temperature of 50 °C was positioned underneath the carbon fabric in order to aid the evaporation of solvent. After spray coating, the solvent was evaporated and the GnPs were immobilized on the fiber surface of carbon fibers. The amount of GnPs that immobilized on carbon fibers was calculated based on the weight of fibers before and after spraying.

The vacuum-assisted resin infusion (VARI) process was carried out to fully infiltrate the fabrics preform. Specifically, eight plies of carbon fabrics immobilized with or without GnPs were stacked unidirectionally and placed in a mold, and then, the laminates were

consolidated in a vacuum bag. The epoxy resin system infused into the fabrics preform via the permeable medium under 0.1 MPa vacuum pressure using a vacuum pump at ambient temperature. After the infiltration of epoxy resins, the impregnated preform was further subjected to hot press at 80 °C for 2 h followed by 5 h at 100 °C under 10 MPa pressure to cure the composite laminates. The final GnPs concentration within the composites was calculated based on the amount of GnPs immobilized on carbon fabrics, regardless of minor waste during the manufacturing process. Laminates containing 0, 0.1, 0.3 and 0.5 wt% GnPs were obtained at the end of the above procedure. Figure 1 schematically illustrates the entire manufacturing process of the GnPs/carbon fiber/epoxy multiscale composites.

Characterization

Morphology

The morphology of raw materials, GnPs-coated fabrics and the dispersion state of GnPs in the interlaminar region were analyzed with an environmental scanning electron microscopy (FE-SEM, Zeiss Ultra 60). The samples were split teared in-between the failed layers after the ILSS tests, and the fractured surfaces of the specimens were examined with SEM to explore the fiber/matrix interactions. To avoid charging, the specimens were gold coated by tungsten (Modular high vacuum coating system Leica EM MED020) prior to observation. Transmission electron microscope (TEM) analyses were characterized with a JEM 2100F STEM/EDS electron microscope at 200 kV.

Structure characterization

Raman spectra of the GnPs were collected with a Raman spectrometer (Renishaw, system 100, UK) in the range of 500–3500 cm^{-1} with a 785 nm laser as incident light. Results are the average of five Raman measurements. X-ray diffraction (XRD) patterns were recorded on a Bruker D8 Advance diffractometer (Germany) with monochromatized Cu Ka radiation. X-ray photoelectron (XPS) spectroscopy of GnPs was analyzed using a Thermo Fisher Scientific (UK) Multilab-2000 XPS spectrometer.

Flexural properties tests

The bending tests were conducted on an Instron 5943 machine. The three-point flexural tests were performed according to the ASTM D-790 standard. Samples with a dimension of 100 mm × 12.7 mm × 2 mm were cut from the panels, and the span-to-depth ratio was set to 32:1. The samples were tested at a crosshead speed of 1.2 mm/min. At least five samples were tested for each type of composites.

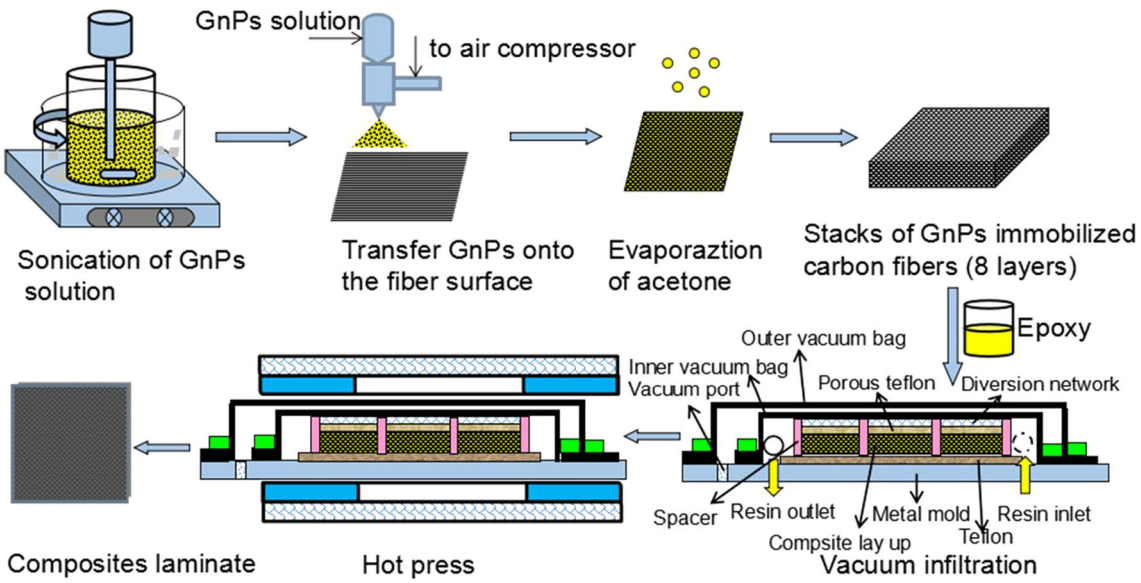

Figure 1 Schematic illustration of GnPs/carbon fiber/epoxy multiscale composites fabrication.

Short-beam shear tests

The three-point short-beam shear (SBS) tests were used to evaluate the influence of GnPs on the ILSS in accordance with ASTM D-2344. The ILSS tests were performed on a MTS Systems Corporation E45.105 machine, and samples with a dimension of 18 mm × 5 mm × 2 mm were prepared. The span-to-depth ratio was set to 4:1, and the test was conducted under displacement control at a displacement rate of 1.2 mm/min. At least five specimens were tested for each composition. The ILSS value (F) was calculated using Eq. (1):

$$F = 0.75\frac{P_{\mathrm{m}}}{bh}, \tag{1}$$

where F = short-beam strength (MPa), P_{m} = maximum load observed during the test (N), b = measured specimen width (mm), and h = measured specimen thickness (mm).

Thermal conductivity tests

The thermal diffusivity of the laminated composites was measured with the laser flash method (LFA 457 NanoFlash) at ambient temperature. Square specimens with a side length of 10 mm were prepared for the measurement of through-plane thermal diffusivity. Graphite was spray-coated on the top and bottom surfaces of the specimens to achieve uniform heat flow and thermal diffusivity (α: mm^2/s), and three measurements were collected. The specific heat capacity (C_{p}: J/g K) was analyzed with DSC (Q2000, TA instruments). The densities (ρ: g/cm^3) of the samples were collected using the drainage method, and a digital micrometer was employed to determine the thickness of the finished samples. The through-plane thermal conductivity of the carbon/epoxy laminates with/without nanoreinforcements was calculated according to Eq. (2):

$$K = \alpha \times \rho \times C_{\mathrm{p}}, \tag{2}$$

where K = thermal conductivity (W/m K), α = thermal diffusivity (mm^2/s), ρ = densities of the samples (g/cm^3), C_{p} = specific heat capacity (J/g K).

Results and discussion

Morphology of GnPs and carbon fibers

Figure 2a illustrates the SEM image of the as-received GnPs. As can be seen, the mean size of GnPs is about 5 μm, which is in accordance with the manufacturer. The SEM image of the neat carbon fibers shown in Fig. 2b reveals a plane, smooth and clean surface. The typical morphology and structure of the GnPs were further observed with TEM, and the images are shown in Fig. 2c, d. As is evident in Fig. 2c, the typical feature of GnPs exhibits a wrinkled surface texture with edges folded up. Furthermore, the high-resolution transmission electron microscopy (HRTEM) image of the GnPs (Fig. 2d) presents the thickness of GnPs (∼ 5 nm), indicating that the GnPs are composed of about 15 such stacked single-layer sheets. The SEM and TEM observations also suggest that the GnPs display a large aspect ratio (∼ 1000). The selected area electron diffraction (SAED) pattern of the GnPs (the inset in Fig. 2d) shows a sixfold symmetric pattern, demonstrating the crystalline structure of GnPs.

Raman, XRD and XPS analysis

To further characterize the structure and composition of the GnPs, the Raman, XRD and XPS analysis were carried out. Figure 3a illustrates the Raman spectrum of the GnPs, the small peak (D band) appeared at 1353 cm^{-1} corresponding to disordered Sp^3-hybridized carbon which are usually induced by mechanical and chemical treatments [33]. Also, a sharp peak (G band) was observed at 1577 cm^{-1} which is associated with in-plane vibrations of the sp^2-hybridized carbon atoms, demonstrating non-defective graphene sheets with well-ordered structure. The low $I_{\mathrm{D}}/I_{\mathrm{G}}$ intensity ratio (0.073) from the spectrum predicts that the GnPs possess a high intrinsic thermal and electrical conductivity. A peak appeared at 2710 cm^{-1} is known to be 2D band, and the intensity of the signal is highly dependent on the layers of GnPs. From the position and shape of the 2D peak, it can be concluded that the GnPs flakes are in a form of multilayer structure.

The XRD pattern of the GnPs is shown in Fig. 3b, and a sharp peak positioned at $2\theta = 26.5°$ was observed. The peak corresponds with a d-spacing of 0.336 nm, which indicates the well-ordered graphitic plane of the GnPs [34]. The XPS spectra are presented in Fig. 4, and Table 1 shows the detailed atomic fraction of GnPs. As shown in Fig. 4a and Table 1, apart from the carbon element, 4.17% oxygen was also detected which indicates that a small amount of oxygen-containing groups present on GnPs.

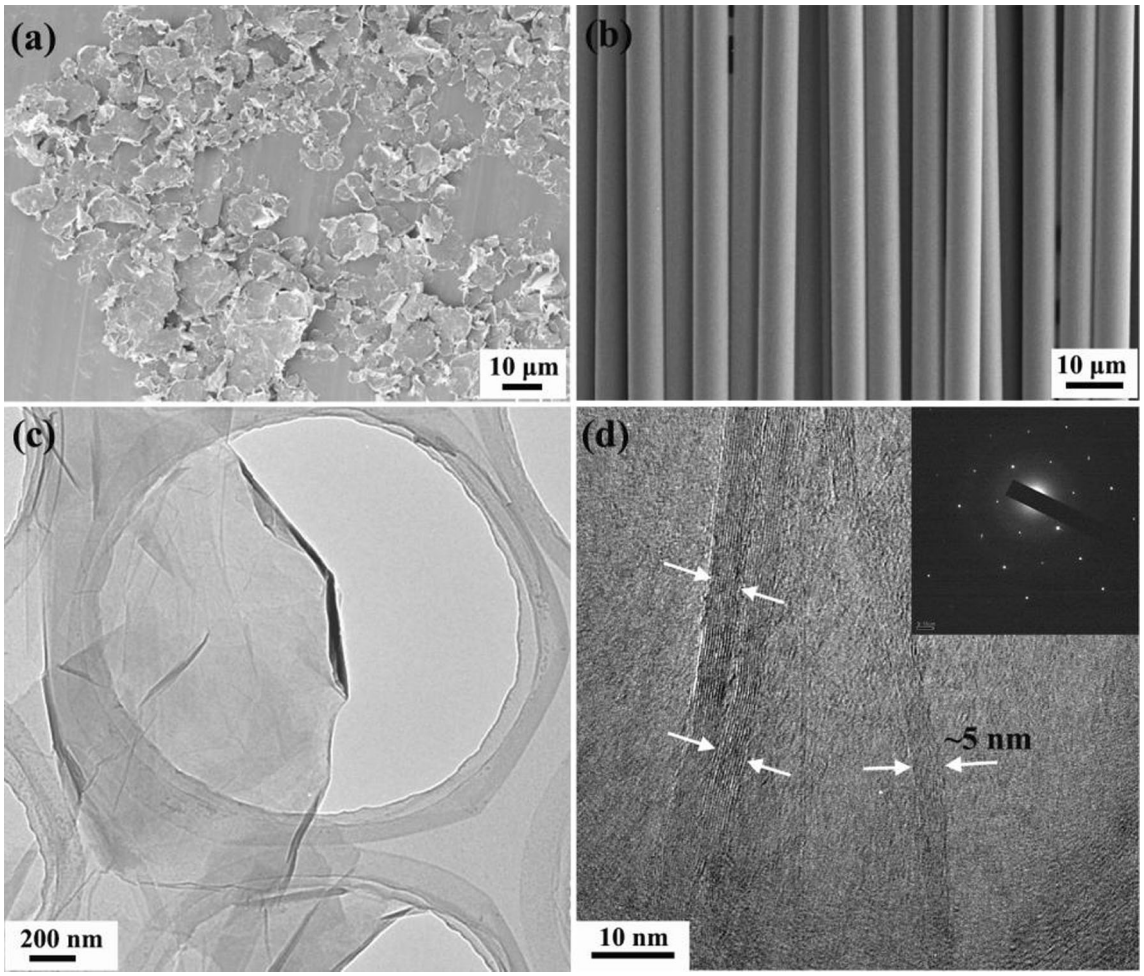

Figure 2 SEM images of **a** GnPs, **b** carbon fiber; and **c** TEM image of GnPs, **d** HRTEM image of GnPs (Insets: the measured electron diffraction pattern).

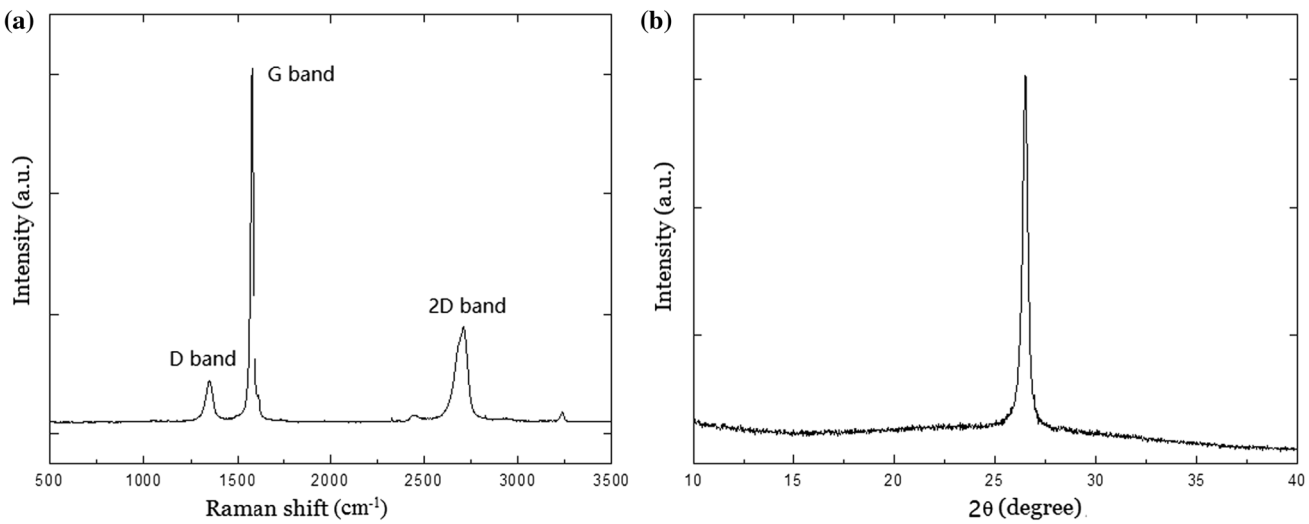

Figure 3 **a** Raman spectrum of GnPs; **b** XRD pattern of GnPs.

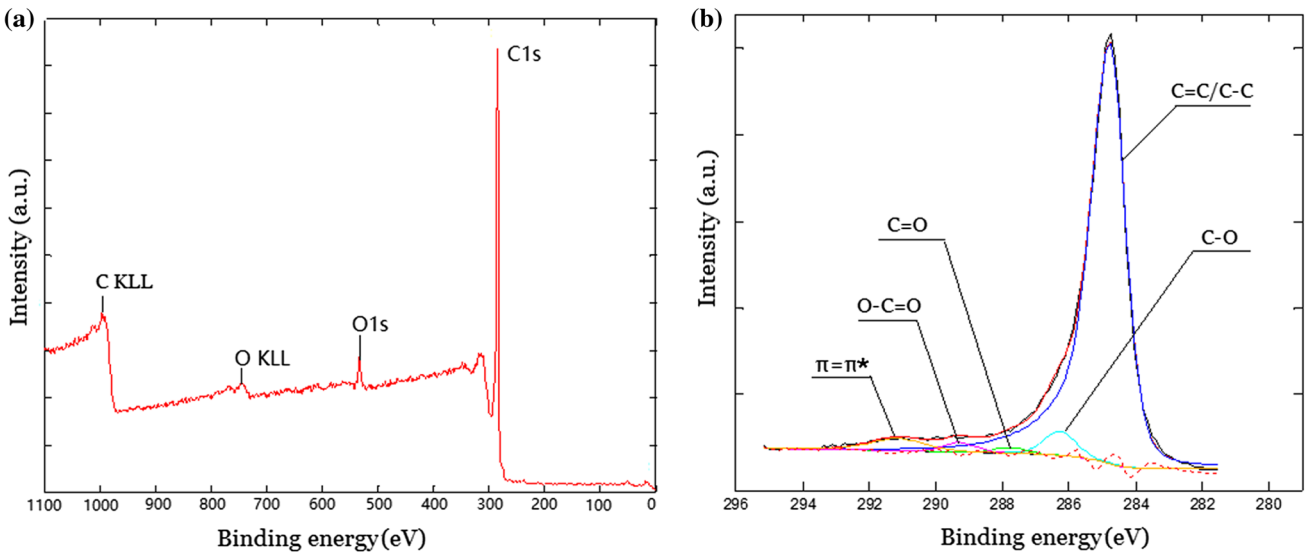

Figure 4 XPS spectra of GnPs: **a** GnPs; **b** Deconvolution of C1s XPS spectrum.

Table 1 Atomic compositions of GnPs based on XPS analysis

Element atomic (%)	C (%)	O (%)	N (%)	C/O (%)
GnPs	95.83	4.17	0	22.98

Furthermore, the detailed information of C1s was also explored. The C1s spectrum of GnPs presented in Fig. 4b shows a major peak at 284.8 eV, which is associated with C=C and C–C in the graphitic structure. Additional peaks appearing at 286.28, 287.78 and 289.28 eV which are assigned to the C atoms functionalized with hydroxyl and epoxy/ether groups, the carbonyl C structure and the carboxylate C, respectively [35]. Apparently, the dominant peak at 284.8 eV confirms the GnPs mostly consists of nonfunctional graphitic structures, but a few retained oxygenic groups with a high carbon-to-oxygen ratio of about 23:1 [36]. Such low oxygenic derivatives enable to address the high thermal and electrical conductivity of the GnPs originated from graphene sheets.

Surface morphology of GnPs-immobilized carbon fibers and GnPs dispersion in composites

The dispersed GnPs solution was sprayed on the surface of the carbon fibers. As the solvent evaporated, a trace amount of epoxy resins remained on fibers act as a binder to anchor GnPs on the fiber surface. The presence of the resins facilitates the GnPs to be well immobilized on the fiber surface and could be able to prevent the formation of agglomerates. The typical SEM image of the GnPs-deposited carbon fibers is depicted in Fig. 5. The 0.1 wt% case (Fig. 5a) shows the presence of GnPs on the fiber surface and among the individual filaments; a magnified SEM image shown in Fig. 5b demonstrates that the GnPs flake is tightly attached and well adhered to the carbon fiber surface. The SEM image of the 0.3 wt% case (Fig. 5c) reveals that more GnPs adhering to carbon fiber surface than that of the 0.1 wt% case, and the GnPs were found to be evenly distributed on the surfaces of carbon fibers. During the subsequent VARI laminate fabrication, the partially cured resin could hold the GnPs on the fabric surface and prevent the GnPs from immigrating, which ensure the even distribution of GnPs in interlaminar regions of the multiscale composites. However, after spraying an excessive amount of GnPs, the GnPs have the tendency to agglomerate as indicated by the black arrows in Fig. 5d (0.5 wt% case) due to strong π–π interplanar stacking resulting from the large specific surface area of GnPs (150 m^2/g) at high GnPs areal density.

To characterize the dispersion of GnPs in the interlaminar region of the composites, a small piece of sample was carefully prepared for SEM observation. Specifically, the sample side with fibers parallelly aligned with each other was polished to be smooth with sandpapers, and then, the polished surface was treated with plasma for 1 h so that the

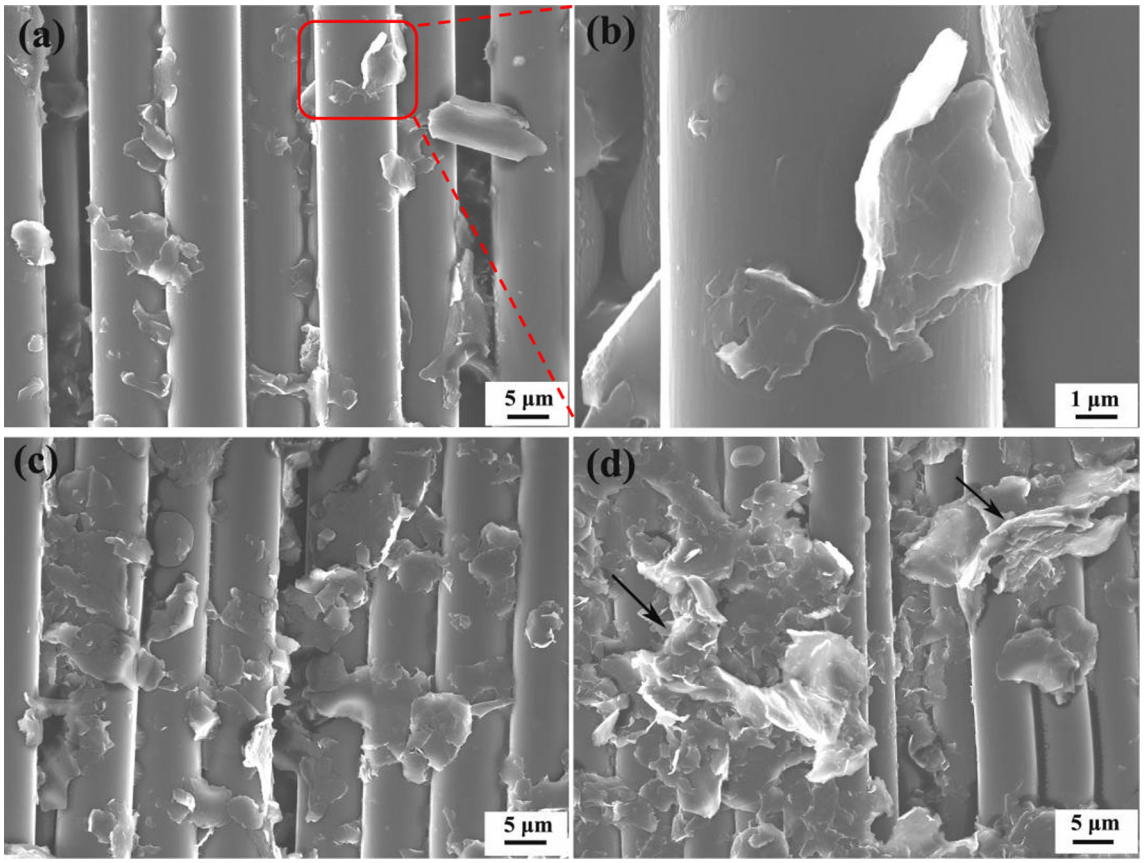

Figure 5 SEM images of GnPs sprayed on the surface of fibers for GnPs/carbon fiber/epoxy composites with different GnPs content: **a** 0.1 wt%, **b** a magnified image showing GnPs well immobilized on fibers, **c** 0.3 wt% and **d** 0.5 wt%.

GnPs can be exposed. Figure 6a shows that the interlaminar matrix of carbon fiber/epoxy composite without any GnPs was etched by plasma, while the GnPs were clearly noticed in the 0.1 wt% GnPs case in Fig. 6b. More GnPs were observed between the interplies in the 0.3 wt% case as indicated by the blue arrows in Fig. 6c. It is noticed that, apart from the GnPs attached to fibers, some of the GnPs orientated along the fiber direction were dispersed in the matrix due to the high pressure and temperature application during the curing. By contrast, agglomerates of GnPs appeared in the 0.5 wt% case as shown in Fig. 6d due to the high GnPs content, which is consistent with the GnPs-immobilized fibers observed in Fig. 5d.

Flexural properties

Figure 7 shows typical flexural load–displacement curves of the GnPs/carbon fiber/epoxy composites with different GnPs concentration. It can be seen that all the curves rise linearly during the early stage of loading and then drop suddenly, confirming the brittle failure mode of epoxy-based laminates. Compared with the curves of the carbon fiber/epoxy composite, the curve of GnPs-reinforced composites demonstrated a larger slope and reached a higher load before catastrophic failure. The introduction of GnPs in the interlaminar region leads to increased energy dissipation, and the laminate with 0.3 wt% GnPs could bear the highest load before failure among all the composites studied.

The summary of flexural modulus and strength results for various GnPs concentration is presented in Fig. 8. As illustrated in Fig. 8a, the flexural modulus was found to pointedly increase with the progressive increase in the content of GnPs, which is resulted from the stiffening effect of the high modulus of rigid GnPs [37–40]. For the flexural strength (Fig. 8b), the pristine specimen yielded a flexural strength value of 757.3 MPa, and the flexural strength was found to be effectively enhanced after the addition of GnPs. At 0.1 and 0.3 wt% GnPs, the flexural strength of the

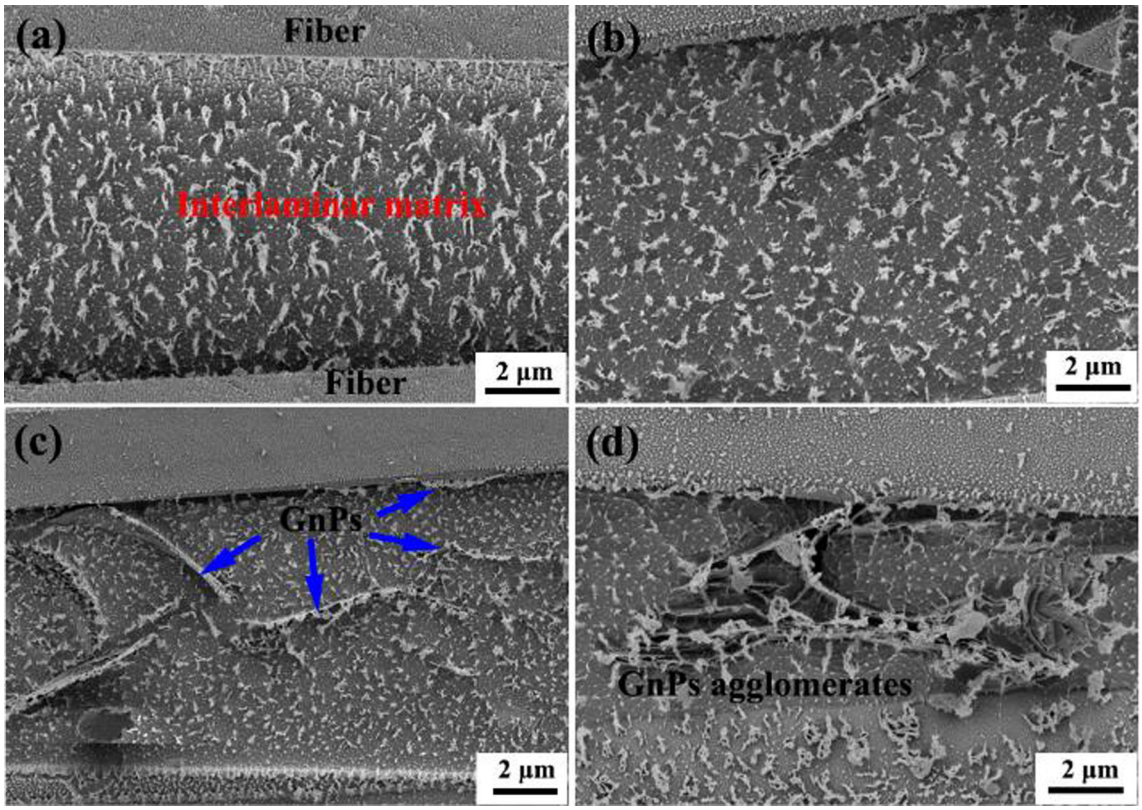

Figure 6 SEM images of the cross section of GnPs/carbon fiber/epoxy composites with different GnPs content: **a** 0 wt%, **b** 0.1 wt%, **c** 0.3 wt% and **d** 0.5 wt%.

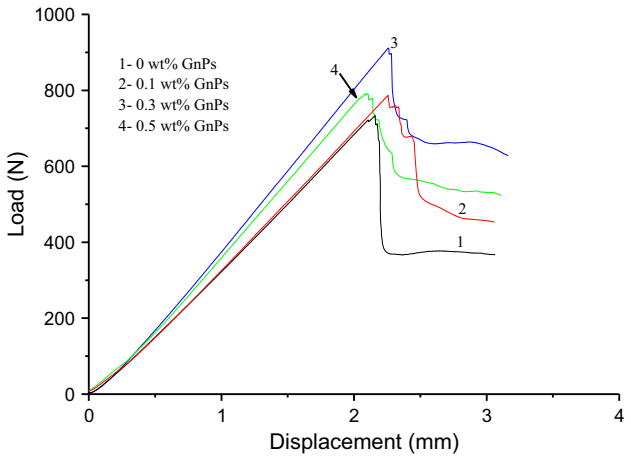

Figure 7 Load–displacement curves obtained from flexural tests of the carbon fiber/epoxy and GnPs/carbon fiber/epoxy multiscale composites.

multiscale nanocomposites reached 848.8 and 963 MPa, corresponding to 12.1% and 27.2% improvements, respectively, compared with that of the control sample. However, when the GnPs content was further increased to 0.5 wt%, the reinforcement effect was less pronounced in comparison with that of the 0.3 wt% case due to agglomerates of GnPs which usually serve as stress concentrators in the interlaminar regions. The evident flexural strength enhancement of the composite with optimum GnPs content (0.3 wt%) is probably ascribed to the fact that the wrinkled structure and high aspect ratio of GnPs that immobilized on the fiber surface improved the fiber/matrix interactions by enhanced mechanical interlocking and interfacial adhesion between fibers and the matrix. Therefore, the strong fiber/matrix interfacial interactions deriving from the evenly distributed GnPs at the interface facilitated load transfer efficiency from the matrix to the carbon fibers, thereby producing higher flexural strength.

It is noteworthy to mention that, the incorporation of optimal content of GnPs leads to 27.2% flexural strength improvement in the present study which is much higher than the enhancement (16.2%) reported in our previous study [41], where GnPs/glass fiber/epoxy multiscale composites were fabricated by impregnating glass fibers with GnPs-modified epoxy mixture. This phenomenon is very interesting, and

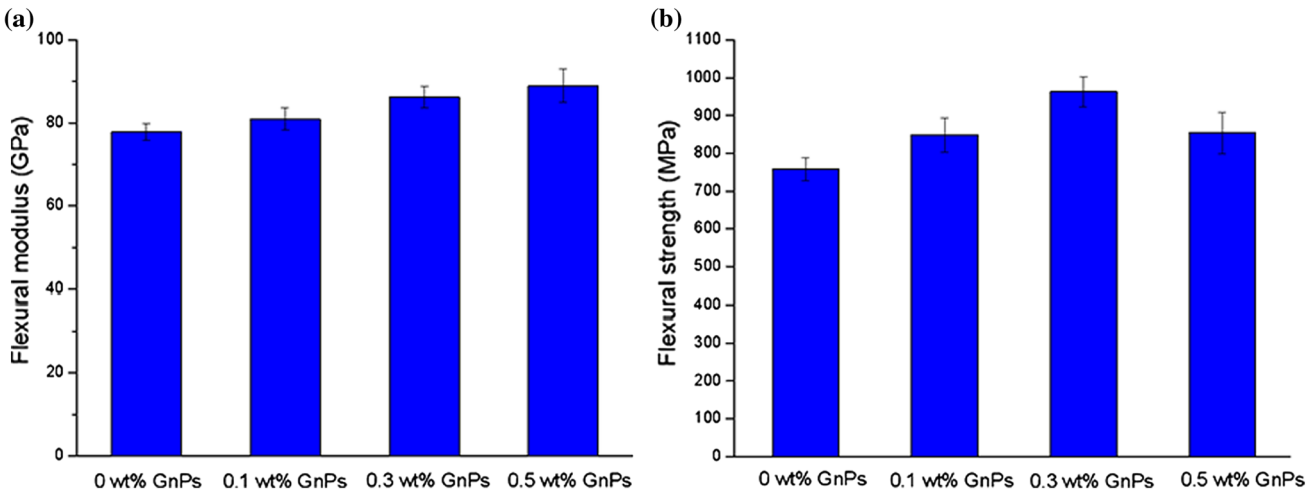

Figure 8 **a** Flexural modulus and **b** strength of the carbon fiber/epoxy and GnPs/carbon fiber/epoxy composites.

the notable improvement reported here might be attributed to the following reasons. In this study, the GnPs were introduced into the CFRP through spraying GnPs on fiber surface instead of mixing GnPs with epoxy resins, which can avoid the formation of GnPs agglomerates at high GnPs content resulting from increased epoxy viscosity. As a consequence, the spraying technique allows GnPs to be evenly immobilized on the fiber surface as shown in Fig. 5c, promoting a stronger reinforcing effect. Moreover, as is known to all, the mechanical strength of fiber-reinforced composites is highly dependent on the fiber/matrix interfacial adhesion, and the interfacial properties could be enhanced by increasing the fiber surface area [42]. The surface area of carbon fibers in this study was locally improved by directly coating the high specific surface area of GnPs (150 m^2/g), which produced a stronger fiber/matrix interfacial interactions. The increased fiber surface area and good interfacial condition might be also beneficial to decrease stress concentration and prevent the cracks directly spreading to the fiber surface. Therefore, moderate amount of GnPs attached to the fiber surface promoted better load transfer, leading to a higher flexural strength enhancement.

When manufacturing flaky fillers-reinforced laminated composites by impregnating fabrics with filler-modified resins, it is usually noticed that the fillers with high aspect ratio, especially the lateral dimension larger than 1 μm, are too large to penetrate into the narrow interstices of fiber bundles and are usually sandwiched between the adjacent fabrics of the resulting hierarchical composites [41]. Therefore, in view of our positive results, it is suggested that alternative facile, efficient and cost-effective approaches should be considered for the selective placement of large dimensional fillers in the susceptible areas of laminated composites to achieve enhanced properties.

Interlaminar shear strength and fracture morphology

It is well known that the interlaminar shear strength (ILSS) of unidirectional composites is function of to the fracture resistance of matrix and fiber/matrix interfacial adhesion strength given the same fiber volume fraction [43]. The ILSS results of the prepared composites are reported in Fig. 9 which exhibits a trend similar to the flexural strength. Compared with the control sample, the average ILSS value increased from 36.7 to 41.5, 45.7 and 44.8 MPa with the GnPs content of 0.1, 0.3 and 0.5 wt%, respectively. Obviously, the largest enhancement was obtained at 0.3 wt% GnPs loading with about a 24.5% improvement. Many researchers have reported that the addition of optimal amount of graphene to an epoxy matrix could significantly improve fracture energy and fatigue crack growth resistance [44–46], and our previous work [23] also showed that the GnPs are effective in enhancing the fracture toughness of polymer composites by preventing micro-crack growth or propagation. Therefore, in the present study, the introduction of GnPs is believed to improve the fracture resistance and toughness of the interfacial regions surrounding the fibers, and the composites could bear higher loading force before laminate

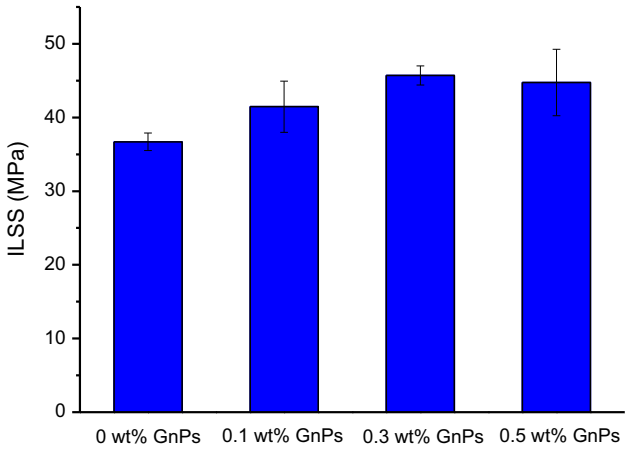

Figure 9 Interlaminar shear strength of the carbon fiber/epoxy and GnPs/carbon fiber/epoxy composites.

failure; thus, a high ILSS of the composites was obtained. In addition, the increase in the ILSS can also be attributed to the strengthening of the interface between the fibers and matrix due to the enhanced mechanical interlocking after immobilizing GnPs on the fiber surface. The wrinkled surface texture of GnPs with high specific surface area enhanced fiber/matrix interfacial interactions and reduced the interlaminar stress concentration, allowing better load transfer from the epoxy matrix to the fibers [16] and thereby increased the composite ILSS. It is noticed that the ILSS enhancement in the present study (24.5%) is lower than the work reported by Shen et al. (32.12%), but higher than that of the Han's work (8.05%) where the fiber laminated composites were fabricated by impregnating fabrics with an epoxy mixture modified with appropriate content of GO [47, 48].

Actually, it is not very scientific to compare GnPs with GO reported in the literature in terms of the reinforcing ability of enhancing ILSS because the reinforcing effect of fillers depends on many factors, such as the filler size, filler content, filler dispersion and the method of adding fillers. However, assuming that all of the above-mentioned factors are the same, it is believed that the GO could perform better in improving the ILSS of fiber laminated composites due to the stronger fiber–filler–matrix interfacial interactions originated from the abundant functional oxygen-containing groups on GO which may bond with epoxy component through chemical bonding [47]. However, the conductive GnPs would be a better choice for the preparation of fiber laminated multiscale composites with desired over-all properties, including mechanical, thermal and electrical properties. The effect of GnPs on the thermal conductivity of the composites will be discussed in the later section.

To investigate the mechanisms of the ILSS enhancements, the specimens were split teared in-between the failed layers after the ILSS tests, and the morphologies of the fractured surfaces of the composites were examined and are presented in Fig. 10. Figure 10a shows that the matrix was completely detached from the non-immobilized fiber surface, and the carbon fibers had very smooth and clean surfaces, illustrating that the interfacial adhesion between fibers and the matrix was relatively weak. The poor interfacial adhesion restrained the load transfer from the matrix to fibers, resulting in the crack initiation and propagation along the interfaces and lowered the ILSS. By contrast, some resin fragments were remained on fiber surface or between the adjacent fibers after incorporating 0.1 wt% GnPs into the composites (Fig. 10b). When cracks form in the composites, the propagation of the cracks can be deflected by the GnPs as indicated by the blue arrows in Fig. 10b. More GnPs were observed in the 0.3 wt% GnPs case as marked by the blue arrows in Fig. 10c, and the inhibition of crack growth induced by the GnPs resulted in more resin fragments attached to the fiber surface, which indicates strong fiber/matrix interfacial interactions. Tearing and peeling of the outer side GnPs layer were also observed as denoted by the black ellipse frames in Fig. 10c. For the 0.5 wt% case, agglomerates of GnPs appeared in the interlaminar region as presented in Fig. 10d. The micro-sized crack might initiate at the GnPs agglomerates and propagate throughout the samples [49], leading to decreased ILSS of the composite in comparison with the composite containing 0.3 wt% GnPs as indicated in Fig. 9.

To further study the reinforcing mechanisms, more SEM images of the fractured surface of composites reinforced with 0.3 wt% were observed and are depicted in Fig. 11. As can be seen, the GnPs with wrinkled morphologies appeared in the interface region as indicated by the blue arrows in Fig. 11a, and the red dashed arrows marked in Fig. 11a and its inset reveal that tearing and peeling of GnPs layers occurred as the crack runs along the GnPs/matrix interface due to the weak interlayer interactions (van der Waals) of GnPs. A high magnification image

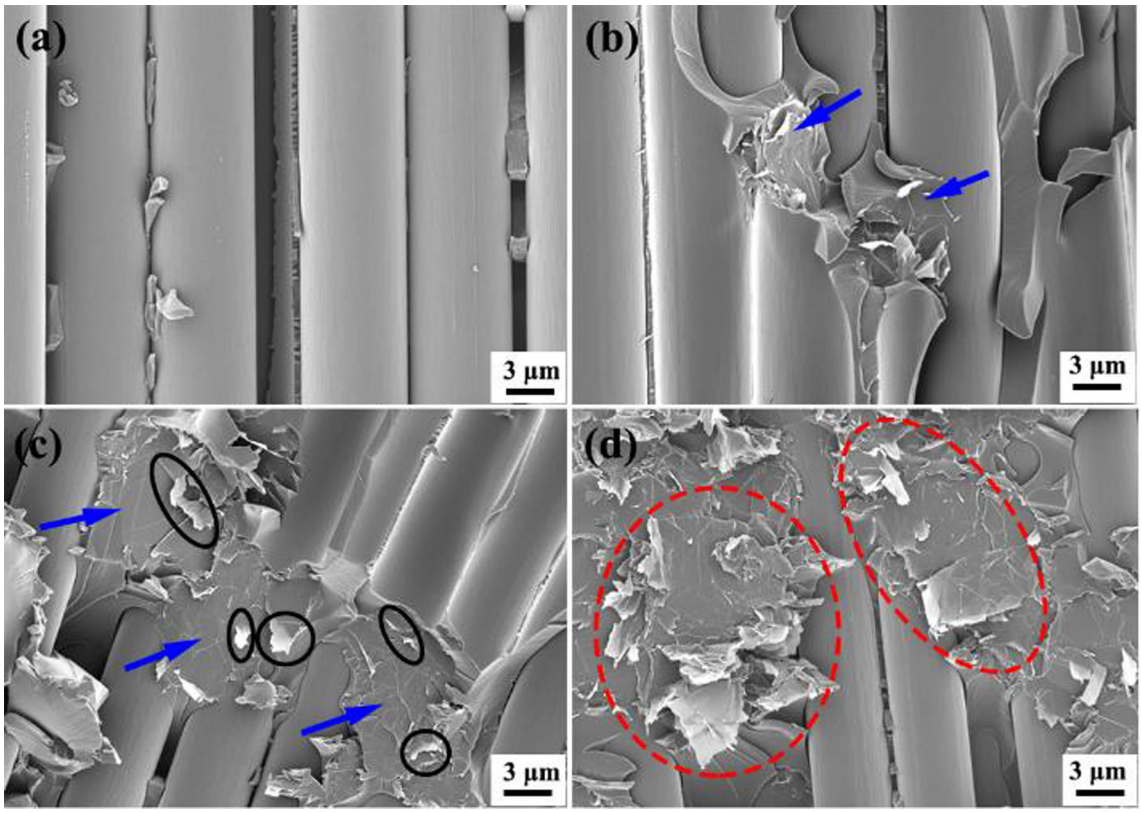

Figure 10 SEM images of the ILSS fracture morphology of GnPs/carbon fiber/epoxy composites with different GnPs content: **a** 0 wt%, **b** 0.1 wt%, **c** 0.3 wt% and **d** 0.5 wt%.

presented in Fig. 11b clearly shows that a thin GnPs layer was peeled from the thicker one with a wrinkled morphology. The tearing and peeling of GnPs layers are commonly seen on GnPs along the fractured surfaces, which could facilitate the shear stress transfer from the matrix to fibers and subsequently improve the ILSS of the composites. Out observations correspond well to Kuo's work [46], in which the tearing and peeling were reported to be the dominant modes of fracture for graphene with layered structures. The blue arrows in Fig. 11c and d show relatively clean surfaces of GnPs, and this might be resulted from the debonding or interlayer separation of the multilayered GnPs due to the weak GnPs/matrix interface and weak interlayer forces of GnPs [23, 45]. The debonding or interlayer separation of GnPs could also dissipate energy during the mechanical tests and subsequently enhanced the ILSS. Moreover, as indicated by the black dashed circles in Fig. 11c, irregular catastrophic fracture surface was also noticed around the GnPs due to the local plastic deformation of matrix promoted by the debonding/separation of GnPs, and a magnified SEM image provided in Fig. 11d clearly shows the dimple structure marked by the dashed blue lines. The formation of the dimple structure resulted in larger fracture areas which could consume larger energy and further contributed to the final high ILSS. Based on the morphology observations, a schematic representation of the failure modes for composites was proposed to help understand the reinforcing mechanisms (Fig. 12).

Thermal conductivity

The thermal conductivity of CFRP is an important property for many applications. It is well known that thermal conductivity is a concept based on phonon transport [50]; introducing conductive fillers into interphase regions of laminated composites would be an effective method to reduce the interlaminar thermal resistivity and enhance the out-of-plane thermal conductivity. For a specific platelet-shape-type filler, the thermal conductivity of composites is highly dependent on the aspect ratio and content of the fillers, and the multilayered GnPs flake with large

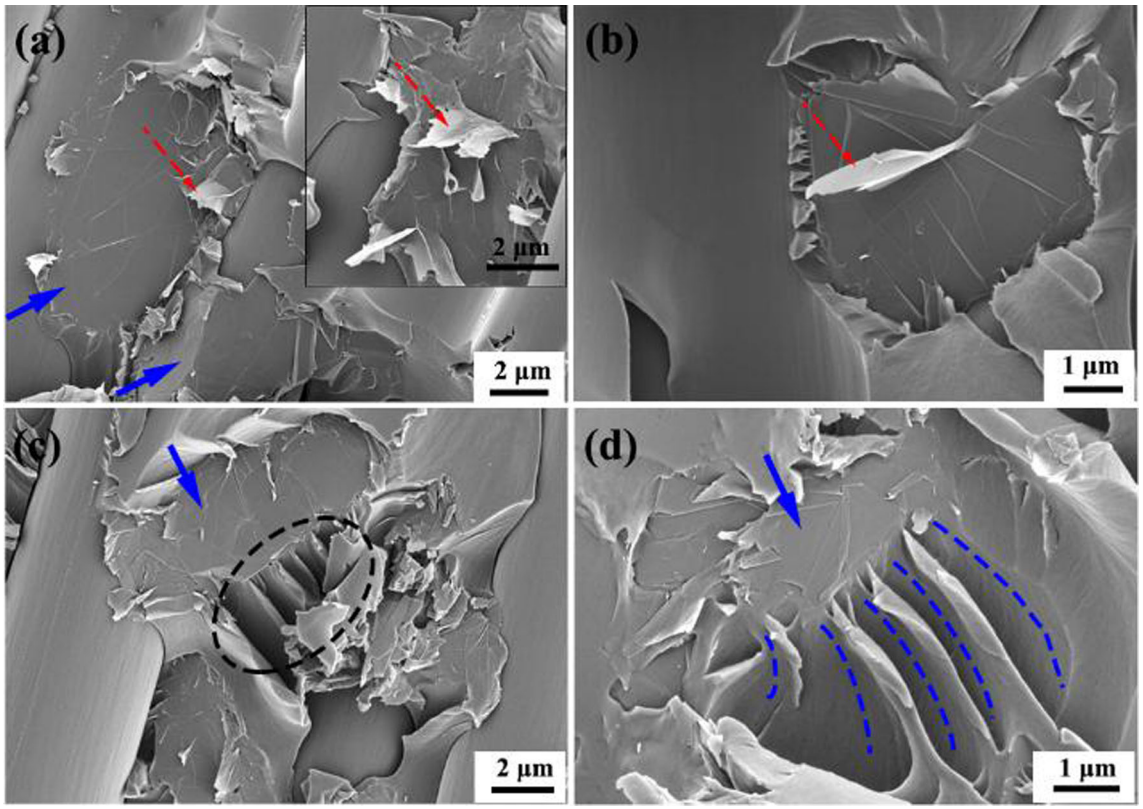

Figure 11 Magnified SEM images of representative fracture surface of the GnPs/carbon fiber/epoxy composite with 0.3 wt% GnPs after ILSS testing.

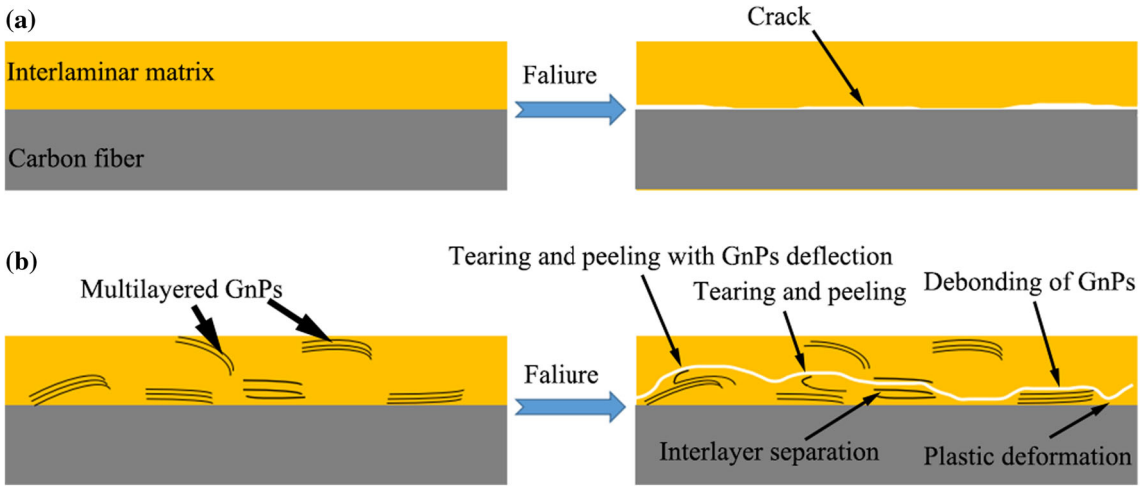

Figure 12 Schematic diagrams of failure mode of **a** pure CFRP and **b** CFRP with GnPs.

lateral size was proven to be an ideal candidate to endow the composites with a good thermal conductivity [22, 23]. Figure 13 shows the through-plane thermal conductivity of composite laminates with various GnPs content. The through-plane thermal conductivity of the GnPs/carbon fiber/epoxy composite laminates increases with the increase in GnPs content. The thermal conductivity of the pristine composites was measured to be 0.54 W/(m K), while the value was increased to 0.84 W/(m K) after the composite reinforced with 0.5 wt% GnPs, which represents a 55.6% increase as compared to the

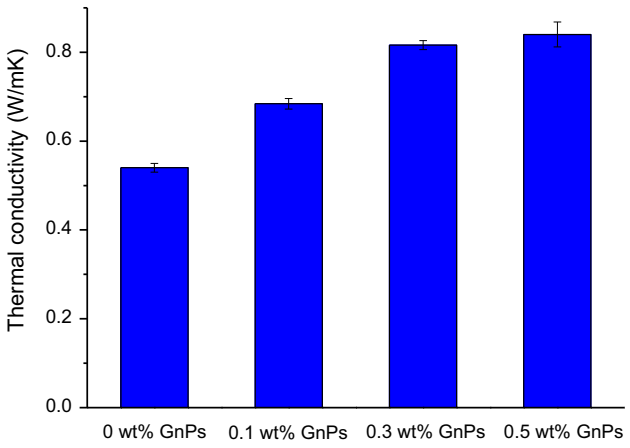

Figure 13 Through-plane thermal conductivity of the GnPs/carbon fiber/epoxy composites.

control sample. The improvement can be attributable to the formation of effective thermal conductive pathways which reduced the thermal resistance between fibers and the matrix and facilitated the phonon diffusion in the through-thickness direction. Moreover, the increase in GnPs content contributed to the increase in GnPs distribution density in the interlaminar region, and more thermal conductive paths were constructed to bridge adjacent fabric plies, generating a high through-plane thermal conductivity of the composites.

Conclusions

In summary, a well-designed spraying technique was employed to introduce GnPs to the surface of carbon fibers with good immobilization, and a potential upscalable approach for manufacturing GnPs-reinforced fiber laminated composites with a hierarchical structure was developed. The flexural properties, ILSS and the thermal conductivity of the resulting composites were carefully studied and evaluated. It has been observed that the introduction of GnPs in the interlaminar regions effectively enhanced the flexural properties and ILSS, and the optimum GnPs content was recorded at 0.3 wt%. The improved flexural properties of the resulting composites can be ascribed to the evenly spread of GnPs that immobilized on the fiber surface which induced strong interfacial interactions between fibers and the matrix. The enhancement of ILSS was mainly resulted from the improved fracture resistance of interfacial regions surrounding fibers and the enhanced fiber/matrix interfacial interactions after the incorporation of GnPs. Moreover, the addition of GnPs improved the through-plane thermal conductivity of the fiber laminated composites by forming effective conductive pathways. Therefore, the facial spraying technique combined with the economical VARI process in this study provided a potential efficient and upscalable route for developing GnPs/fiber/epoxy multiscale composites with enhanced mechanical performance and thermal conductivity.

Acknowledgements

The authors acknowledge the financial support from Science Foundation of Shandong Province, China (Grant No. ZR2017QEM001).

Compliance with ethical standard

Conflicts of interest The authors declare that they have no conflicts of interest.

References

[1] Chand S (2000) Carbon fibers for composites. J Mater Sci 35:1303–1313. https://doi.org/10.1023/A:1004780301489

[2] Chae HG, Kumar S (2008) Materials science-making strong fibers. Science 319:908–909

[3] Mirjalili V, Ramachandramoorthy R, Hubert P (2014) Enhancement of fracture toughness of carbon fiber laminated composites using multi wall carbon nanotubes. Carbon 79:413–423

[4] Kandare E, Khatibi AA, Yoo S, Wang RY, Ma J, Olivier P, Gleizes N, Wang CH (2015) Improving the through-thickness thermal and electrical conductivity of carbon fibre/epoxy laminates by exploiting synergy between graphene and silver nano-inclusions. Compos Part A Appl Sci Manuf 69:72–82

[5] Liu Y, Yang JP, Xiao HM, Qu CB, Feng QP, Fu SY, Shindo Y (2012) Role of matrix modification on interlaminar shear strength of glass fibre/epoxy composites. Compos Part B Eng 43:95–98

[6] Haghbin A, Liaghat GH, Arabi AM, Hadavinia H, Pol MH (2018) Investigations on electrophoretic deposition of carbon nanotubes on glass textures to improve polymeric composites interface. Compos Sci Technol 155:197–204

[7] Guo J, Zhang QJ, Gao L, Zhong WH, Sui G, Yang XP (2017) Significantly improved electrical and interlaminar mechanical properties of carbon fiber laminated composites

by using special carbon nanotube pre-dispersion mixture. Compos Part A Appl Sci Manuf 95:294–303

[8] El Moumen A, Tarfaoui M, Lafdi K, Benyahia H (2017) Dynamic properties of carbon nanotubes reinforced carbon fibers/epoxy textile composites under low velocity impact. Compos Part B Eng 125:1–8

[9] El Moumen A, Tarfaoui M, Lafdi K (2017) Mechanical characterization of carbon nanotubes based polymer composites using indentation tests. Compos Part B Eng 114:1–7

[10] Tarfaoui M, Lafdi K, El Moumen A (2016) Mechanical properties of carbon nanotubes based polymer composites. Compos Part B Eng 103:113–121

[11] El Moumen A, Tarfaoui M, Hassoon O, Lafdi K, Benyahia H, Nachtane M (2018) Experimental study and numerical modelling of low velocity impact on laminated composite reinforced with thin film made of carbon nanotubes. Appl Compos Mater 25:309–320

[12] El Moumen A, Tarfaoui M, Lafdi K (2018) Computational homogenization of mechanical properties for laminate composites reinforced with thin film made of carbon nanotubes. Appl Compos Mater 25:569–588

[13] Lee C, Wei X, Kysar JW, Hone J (2008) Measurement of the elastic properties and intrinsic strength of monolayer graphene. Science 321:385–388

[14] Balandin AA, Ghosh S, Bao W, Calizo I, Teweldebrhan D, Miao F, Lau CN (2008) Superior thermal conductivity of single-layer graphene. Nano Lett 8:902–907

[15] Du X, Skachko I, Barker A, Andrei EY (2008) Approaching ballistic transport in suspended graphene. Nat Nanotechnol 3:491–495

[16] Zhang X, Fan X, Yan C, Li H, Zhu Y, Li X, Yu L (2012) Interfacial microstructure and properties of carbon fiber composites modified with graphene oxide. ACS Appl Mater Interfaces 4:1543–1552

[17] Adak NC, Chhetri S, Murmu NC, Samanta P, Kuila T, Lee JH (2019) Experimental and numerical investigation on the mechanical characteristics of polyethylenimine functionalized graphene oxide incorporated woven carbon fibre/epoxy composites. Compos Part B Eng 156:240–251

[18] Hung PY, Lau KT, Fox B, Hameed N, Lee JH, Hui D (2018) Surface modification of carbon fibre using graphene–related materials for multifunctional composites. Compos Part B Eng 133:240–257

[19] Drzal LT, Fukushima H (2006) Expanded graphite and products produced therefrom. U.S. Patent (US 8501858 B2)

[20] Wang FZ, Drzal LT, Qin Y, Huang ZX (2015) Multifunctional graphene nanoplatelets/cellulose nanocrystals composite paper. Compos Part B Eng 79:521–529

[21] Wang FZ, Drzal LT, Qin Y, Huang ZX (2015) Mechanical properties and thermal conductivity of graphene nanoplatelets/epoxy nanocomposites. J Mater Sci 50:1082–1093. https://doi.org/10.1016/j.cplett.2012.02.006

[22] Shen X, Wang ZY, Wu Y, Liu X, He YB, Kim JK (2016) Multilayer graphene enables higher efficiency in improving thermal conductivities of graphene/epoxy composites. Nano Lett 16:3585–3593

[23] Wang FZ, Drzal LT, Qin Y, Huang ZX (2016) Enhancement of fracture toughness, mechanical and thermal properties of rubber/epoxy composites by incorporation of graphene nanoplatelets. Compos Part A Appl Sci Manuf 87:10–22

[24] Ahmadi-Moghadam B, Taheri F (2014) Effect of processing parameters on the structure and multi-functional performance of epoxy/GNP-nanocomposites. J Mater Sci 49:6180–6190. https://doi.org/10.1007/s10853-014-8332-y

[25] Qin WZ, Vautard F, Drzal LT, Yu JR (2015) Mechanical and electrical properties of carbon fiber composites with incorporation of graphene nanoplatelets at the fiber-matrix interphase. Compos Part B Eng 69:335–341

[26] Ahmadi-Moghadam B, Taheri F (2015) Influence of graphene nanoplatelets on modes I, II and III interlaminar fracture toughness of fiber-reinforced polymer composites. Eng Fract Mech 143:97–107

[27] Zhang KM, Gu YZ, Li M, Zhang ZG (2014) Effect of rapid curing process on the properties of carbon fiber/epoxy composite fabricated using vacuum assisted resin infusion molding. Mater Des 54:624–631

[28] Bender D, Schuster J, Heider D (2006) Flow rate control during vacuum-assisted resin transfer molding (VARTM) processing. Compos Sci Technol 66:2265–2271

[29] Zhang H, Liu Y, Huo SS, Briscoe J, Tu W, Picot OT, Rezai A, Bilotti E, Peijs T (2017) Filtration effects of graphene nanoplatelets in resin infusion processes: Problems and possible solutions. Compos Sci Technol 139:138–145

[30] Shan FL, Gu YZ, Li M, Liu NY, Zhang ZG (2013) Effect of deposited carbon nanotubes on interlaminar properties of carbon fiber-reinforced epoxy composites using a developed spraying processing. Polym Compos 34:41–50

[31] Adak NC, Chhetri S, Kuila T, Murmu NC, Samanta P, Lee JH (2018) Effects of hydrazine reduced graphene oxide on the inter-laminar fracture toughness of woven carbon fiber/epoxy composite. Compos Part B Eng 149:22–30

[32] Jia JJ, Du XS, Chen C, Sun XY, Mai YW, Kim JK (2015) 3D network graphene interlayer for excellent interlaminar toughness and strength in fiber reinforced composites. Carbon 95:978–986

[33] Wang FZ, Drzal LT, Qin Y, Huang ZX (2016) Effects of functionalized graphene nanoplatelets on the morphology and properties of epoxy resins. High Perform Polym 28:1–7

[34] Li F, Liu Y, Qu CB, Xiao HM, Hua Y, Sui GX, Fu SY (2015) Enhanced mechanical properties of short carbon fiber

reinforced polyethersulfone composites by graphene oxide coating. Polymer 59:155–165

[35] Stankovich S, Dikin DA, Piner RD, Kohlhaas KA, Kleinhammes A, Jia Y, Wu Y, Nguyen ST, Ruoff RS (2007) Synthesis of graphene-based nanosheets via chemical reduction of exfoliated graphite oxide. Carbon 45:1558–1565

[36] Zhang Q, Xu X, Li H, Xiong G, Hu H, Fisher TS (2015) Mechanically robust honeycomb graphene aerogel multifunctional polymer composites. Carbon 93:659–670

[37] Halpin J (1969) Stiffness and expansion estimates for oriented short fiber composites. J Compos Mater 3:732–734

[38] Mori T, Tanaka K (1973) Average stress in matrix and average elastic energy of materials with misfitting inclusions. Acta Metall 21:571–574

[39] Cox H (1952) The elasticity and strength of paper and other fibrous materials. Br J Appl Phys 3:72–79

[40] Gao XL, Li K (2005) A shear-lag model for carbon nanotube-reinforced polymer composites. Int J Solids Struct 42:1649–1667

[41] Wang FZ, Drzal LT, Qin Y, Huang ZX (2016) Size effect of graphene nanoplatelets on the morphology and mechanical behavior of glass fiber/epoxy composites. J Mater Sci 51:3337–3348. https://doi.org/10.1007/s10853-015-9649-x

[42] Zhang RL, Gao B, Du WT, Zhang J, Cui HZ, Liu L, Ma QH, Wang CG, Li FH (2016) Enhanced mechanical properties of multiscale carbon fiber/epoxy composites by fiber surface treatment with graphene oxide/polyhedral oligomeric silsesquioxane. Compos Part A Appl Sci Manuf 84:455–463

[43] Khan SU, Kim JK (2012) Improved interlaminar shear properties of multiscale carbon fiber composites with bucky paper interleaves made from carbon nanofibers. Carbon 50:5265–5277

[44] Rafiee MA, Rafiee J, Srivastava I, Wang Z, Song H, Yu ZZ, Koratkar N (2010) Fracture and fatigue in graphene nanocomposites. Small 6:179–183

[45] Chandrasekaran S, Sato N, Tölle F, Mülhaupt R, Fiedler B, Schulte K (2014) Fracture toughness and failure mechanism of graphene based epoxy composites. Compos Sci Technol 97:90–99

[46] Kuo WS, Tai NH, Chang TW (2013) Deformation and fracture in graphene nanosheets. Compos Part A Appl Sci Manuf 51:56–61

[47] Shen XJ, Meng LX, Yan ZY, Sun CJ, Ji YH, Xiao HM, Fu SY (2015) Improved cryogenic interlaminar shear strength of glass fabric/epoxy composites by graphene oxide. Compos Part B Eng 73:126–131

[48] Yang JP, Yang G, Xu GH, Fu SY (2007) Cryogenic mechanical behaviors of MMT/epoxy nanocomposites. Compos Sci Technol 67:2934–2940

[49] Han X, Zhao Y, Sun JM, Li Y, Zhang JD, Hao Y (2017) Effect of graphene oxide addition on the interlaminar shear property of carbon fiber-reinforced epoxy composites. New Carbon Mater 32:48–55

[50] Nika DL, Balandin AA (2017) Phonons and thermal transport in graphene and graphene-based materials. Rep Prog Phys 80:036502